Soft Matter

Damage in elastomers: Healing of internally nucleated cavities and micro-cracks

Journal:	*Soft Matter*
Manuscript ID	SM-ART-02-2018-000238.R2
Article Type:	Paper
Date Submitted by the Author:	01-May-2018
Complete List of Authors:	Poulain, Xavier; University of Texas at Austin, Aerospace Engineering Lopez-Pamies, Oscar; University of Illinois Ravi-Chandar, Krishnaswamy; University of Texas at Austin, Aerospace Engineering

Soft Matter

PAPER TYPE

Cite this: DOI: 10.1039/xxxxxxxxxx

Damage in elastomers: Healing of internally nucleated cavities and micro-cracks

Xavier Poulain,[a] Oscar Lopez-Pamies,[b] and K. Ravi-Chandar[a]

Received Date
Accepted Date

DOI: 10.1039/xxxxxxxxxx

www.rsc.org/journalname

Following on the work of Poulain et al. (Damage in elastomers: Nucleation and growth of cavities, micro-cracks, and macro-cracks. *International Journal of Fracture* 2017, **205**, 1–21.), this paper presents an investigation of the response of cavities/cracks internally nucleated within a transparent PDMS elastomer that is confined between two firmly embedded stiff beads and subjected to quasistatic cyclic loading-unloading. Specifically, it is observed that cracks that nucleate and propagate to reach tens of microns in length during the loading can heal completely upon unloading. They do so autonomously within a time scale of seconds. Furthermore, the regions of the elastomer that experience healing appear to acquire higher strength or toughness.

1 Introduction

As part of an on-going experimental and theoretical program to fathom the fundamental processes of nucleation and propagation of fracture in elastomers undergoing large quasistatic deformations, Poulain et al.[1] have reproduced the classical experiments of Gent and Park[2]. Specifically, blocks of transparent polydimethylsiloxane (PDMS) elastomer of various compositions were filled by two stiff spherical beads of millimetric diameter D separated by an initial submillimetric gap H, and subjected to quasistatic stretching along the line connecting the centers of the spherical beads in an effort to systematically examine the nucleation — a process commonly referred to in the literature as *cavitation* — and growth of internal cavities/cracks within the PDMS region between the beads. The key new ingredients in that work were the addition, in the experiments, of high spatiotemporal resolution (of 1 μm in space and 66.7 ms in time) imaging, and the accounting, in the analysis, of an appropriate constitutive model for the PDMS and of the precise specimen geometry and applied loading conditions.

The use of high spatiotemporal resolution imaging, in conjunction with the associated theoretical analysis, led to a plurality of new observations and these to a number of significant conclusions, perhaps most notably, that *the onset of cavitation in elastomers is a by-product of fracture and not solely of elasticity*. In particular, a general *elastic* criterion*, stating that inside an elastomer with initial shear modulus μ cavitation can first occur at material points where the principal Cauchy stresses t_i $(i = 1,2,3)$ satisfy the condition[5]

$$8t_1t_2t_3 - 12\mu(t_1t_2 + t_2t_3 + t_3t_1) + 18\mu^2(t_1 + t_2 + t_3) - 35\mu^3 = 0 \quad (1)$$

with $t_i > 3\mu/2$ was shown through experiments to be underpredictive (see Fig. 7 in Poulain et al.[1]). The associated numerical analyses of the elastic expansion of pre-existing cavities/cracks further pointed to the fact that such a lack of predictability was precisely because the onset of cavitation in all the various PDMS elastomers studied in Poulain et al.[1] depended *fundamentally* on their non-Gaussian stiffening at large stretches and, more significantly, on their fracture properties. These results have brought resolution to the competing views of Gent and Lindley[4], who viewed cavitation as an elastic instability, and of Williams and Schapery[6], who viewed cavitation as a fracture process: fracture *is* an essential part of the nucleation of cavities/cracks in elastomers.

Another of the key observations reported in Poulain et al.[1] is that the cracks internally nucleated within the various PDMS elastomers might completely *heal*, even after they had grown to reach several tens of microns in length scale. Indeed, for the cases where there were multiple nucleation of cavities/cracks, with continued loading, one of the cracks continued to grow to macroscopic dimensions (reaching hundreds of microns or even larger dimensions) while the remaining cracks were unloaded, and disappeared from view. A good example of this can be seen in Fig. 9 of Poulain et al.[1], where as the crack near the left bead

[a] *Center for Mechanics of Solids, Structures, and Materials Department of Aerospace Engineering and Engineering Mechanics, University of Texas at Austin, TX 78712-1221; E-mail: ravi@utexas.edu*

[b] *Department of Civil and Environmental Engineering, University of Illinois, Urbana–Champaign, IL 61801, USA; E-mail: pamies@illinois.edu*

* We recall (see Section 5 in Lopez-Pamies et al.[3]) that the criterion (1) corresponds to a generalization of the classical elastic cavitation criterion of Gent and Lindley[4] that applies: (*i*) to elastomers that contain a random isotropic distribution of vacuous defects (as opposed to just a single spherical vacuous defect) and (*ii*) arbitrary loadings (as opposed to just purely hydrostatic loading).

continues to grow, the one near the right bead shrinks, and in the unloaded state is not optically visible. The purpose of this paper — which is a continuation of the work of Poulain et al.[1] — is to investigate the closing of such micro-cracks and, in particular, if and how healing occurs. We will do so through carefully designed experiments consisting in cyclically loading-unloading the same type of specimens used in Poulain et al.[1].

The organization of this paper is as follows. In Section 2, the techniques used to prepare the specimens and the experimental schemes used for observation and characterization of the nucleation and propagation of fracture and healing are summarized. The sequence of events beginning with nonlinear deformation, continuing through the first nucleation of a cavity/crack, followed by the subsequent nucleation and growth of multiple cracks, their subsequent unloading, healing, and reloading response are described in detail in Section 3 for a representative specimen. A discussion of the physical processes that could contribute to the observed response is presented in Section 4. Finally, Section 5 is devoted to summarizing the main findings of this work.

2 Experimental design for microscopic observations

The details of specimen preparation are described in Poulain et al.[1]. In this section, for completeness, we provide a brief summary. The PDMS used in this study was made from Dow Corning Sylgard 184 silicone elastomer base with its associated curing agent. In this work, we designed two-bead specimens similar to those of Gent and Park[2] with the aim of inducing cavitation within the PDMS confined between the two beads, where the stress field was controlled by varying the cross-link density of the PDMS (essentially by varying the ratio of base to curing agent), the diameter of the beads D, and the initial distance between the beads H. Since the beads were fully embedded into the PDMS and placed close to each other, there was enough elastomer in the transverse directions to neglect any free surface effects on the fracture/healing mechanisms; this was confirmed to be in fact the case by numerical simulations. The selected geometry for the specimens also allowed a full examination of the crack propagation after very large overall deformations and beyond the domain of interaction between the beads. A sketch of the geometry of the specimens used is shown in Fig. 1.

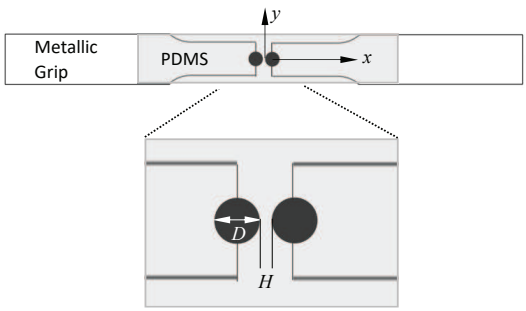

Fig. 1 Schematic of a specimen in the undeformed configuration. The inset shows the two beads of diameter D, separated by a gap H.

While the manufacturer's recommendation is to use the PDMS base and curing agent in the ratio of 10:1, as also done in Poulain et al.[1], we prepared different mixtures. The results reported in Section 3 correspond to a ratio of 30:1. The base and curing agent were poured into a plastic cup, stirred for 15 min, and then degassed for about 30 min. Meanwhile, the spherical beads were cleaned successively in alcohol and acetone, and then coated with a thin layer of Dow Corning 92-023 primer. A specimen mold was made with polymer sheets; a glass microscope slide was placed at the bottom in order to improve transparency and surface finish; all surfaces were coated with a release agent for ease of removal of the specimen. The end grips with the beads attached were then placed on top of the glass slide with appropriate spacing between the glass beads; the degassed PDMS mixture was poured in the mold to form the appropriate thickness. The mold was placed in an oven for curing at 80 °C for about 12 hours before demolding and cutting to shape.

Prior to testing, in order to determine the quasistatic elastic response of the specific PDMS under investigation, a uniaxial tensile test was performed on a rectangular strip specimen, with a self-tightening grip, at a constant stretch rate of 10^{-3} s^{-1}. Digital Image Correlation (DIC) was used to determine the local and global stretches in the gauge section of the specimen. The variation of the nominal stress with the stretch is described in Poulain et al.[1]. The rubber-elastic response, including non-Gaussian stiffening at large stretches, of this composition of PDMS was evident. This is an indication that the use of a smaller weight fraction of crosslinking agent than that recommended by the manufacturer — specifically, again, a 30:1 ratio of base to curing agent *vs* the recommended 10:1 ratio —- still results in a solid with rubbery response, albeit one with a smaller cross-link density. What is not evident is whether there are untethered polymer chains still remaining within the cross-linked network. In order to probe the presence and possible role of these chains, we performed two types of further experiments. First, cyclic loading-unloading uniaxial tension experiments were performed at constant stretch rates in the range of $|\dot{\lambda}| = 2\times10^{-4}$ s^{-1} to 2×10^{-1} s^{-1} up to reaching a maximum stretch level of $\lambda = 2.5$. To within measurement error, the response was observed to be elastic and exhibited no hysteresis. Second, relaxation experiments were also performed in which the specimens were uniaxially stretched at a constant stretch rate of $\dot{\lambda} = 2\times10^{-3}$ s^{-1} up to a stretch between $\lambda = 1.4$ and 2.3, and then held for times between 5 and 15 hours. To within measurement error, no load relaxation was observed. These two types of experiments were performed on specimens that had been synthesized 15 months prior to being tested, as well as on specimens that were newly manufactured and tested after 24 hours. The lack of hysteretic behavior or relaxation implies that the PDMS compositions† tested behave essentially as nonlinear elastic solids, and could be interpreted further as indication that the role of any untethered chains is imperceptible in

† PDMS elastomers with compositions 10:1 and 45:1 were also evaluated through the same protocol. Much like the PDMS elastomer with 30:1 composition, to within measurement error, they exhibited no hysteretic behavior and no relaxation.

the macroscocpic response of such PDMS elastomers. We refer the interested reader to Section 2b in Chapter XI of the monograph by Flory[7] for a discussion of how variations in the number of cross-links and the presence of untethered polymer chains might affect the macroscopic rubber-elastic response of the elastomer. At any rate, as expected, the elastic responses of the different PDMS compositions could not be characterized as simply Neo-Hookean beyond moderate levels of stretch because of their non-Gaussian stiffening at large stretches. They could be accurately and easily characterized, however, by the incompressible hyperelastic model introduced by Lopez-Pamies[8]. In this model, the stored-energy function is given by

$$W(\mathbf{F}) = \begin{cases} \dfrac{3^{1-\alpha_1}}{2\alpha_1}\mu_1\left[I_1^{\alpha_1} - 3^{\alpha_1}\right] + \dfrac{3^{1-\alpha_2}}{2\alpha_2}\mu_2\left[I_1^{\alpha_2} - 3^{\alpha_2}\right] & \text{if } \det\mathbf{F} = 1 \\ +\infty & \text{otherwise} \end{cases}, \tag{2}$$

where $I_1 = F_{ij}F_{ij}$ stands for the standard first principal invariant associated with the deformation gradient tensor $\mathbf{F}$ and $\mu_1, \mu_2, \alpha_1, \alpha_2$ are material constants. The material constants calibrated for the PDMS elastomer with composition 30:1 are given in Table 1.

Table 1 Lopez-Pamies Material Model Coefficients

PDMS composition	α_1	α_2	μ_1 (MPa)	μ_2 (MPa)
30:1	-1.02103	1.39107	0.01857	0.03192

Also prior to testing, high-resolution images of the specimens were taken with the help of a Keyence Model VHX 5000 optical microscope in order to determine the bead diameter and the gap between the beads accurately. Imperfections both in the PDMS matrix (specifically, fabrication induced voids and specimen surface waviness) and on the surfaces of the beads were also examined. These images corresponding to the undeformed specimens in their original configurations were critical since they were used as the reference for both deformation measures and for identification of cavity/crack nucleation should the transparency not be optimal.

The specimens were gripped at both ends on a testing machine (MTII Fullam SEM test frame; see Fig. 3 of Poulain et al.[1]), and the test machine placed under the Keyence Model VHX 5000 microscope. The specimens were loaded in tension at a quasistatic constant displacement rate of 5 mm/min. The loading-unloading-reloading protocol was introduced manually; in particular, as soon as the nucleation of a cavity/crack was observed, the direction of the test machine was reversed in order to stop further growth of the damage, and to unload it. Unloading proceeded until the initial gap between the beads was restored. This was then followed by similar loading-unloading cycles until final failure in the form of the generation of a macroscopic crack was observed. As it was the case in the experiments reported in Poulain et al.[1], force measurements were of little use since the force remained quite small (typically < 1N) — consistent with the specimen small cross section (2×5 mm^2) — below the resolution of the load cell used. The optical microscope allowed the experiments to be followed at high magnification and to be fully video-recorded with high spatial and temporal resolutions: 1200×1600 pixels, 15 frames/sec, and ten-minute maximum duration. The deformation was observed from the top view with illumination from the bottom; the view observed for the spherical beads would appear as in the sketches of the specimen in Fig. 1. The onset of cavitation could be identified readily from a local change in the image contrast of the PDMS elastomer generated by the occlusion of light by the cavity/crack. This experimental arrangement enabled the capture of the nonlinear deformation process, the first nucleation event, and subsequent deformation and damage mechanisms, the unloading and healing of the damage, and the damage growth leading to final specimen failure.

3 Nucleation, propagation, and healing of fractures in a PDMS elastomer

In the sequel, we report the distinct sequence of events — nucleation, growth, shrinking, healing, and reinitiation of cavities/cracks — observed in a representative specimen with bead diameter $D = 3.170$ mm, gap $H = 0.162$ mm, and PDMS composition of 30:1. These are parameterized in terms of the average stretch $\overline{\lambda}$, defined as the ratio of current-to-initial gap across the beads: $\overline{\lambda} \doteq h/H$. We remark that other tests featuring different gap-to-diameter ratios H/D and PDMS with composition 45:1 exhibited essentially the same sequence of events; tests were not performed on PDMS compositions other than 30:1 and 45:1.

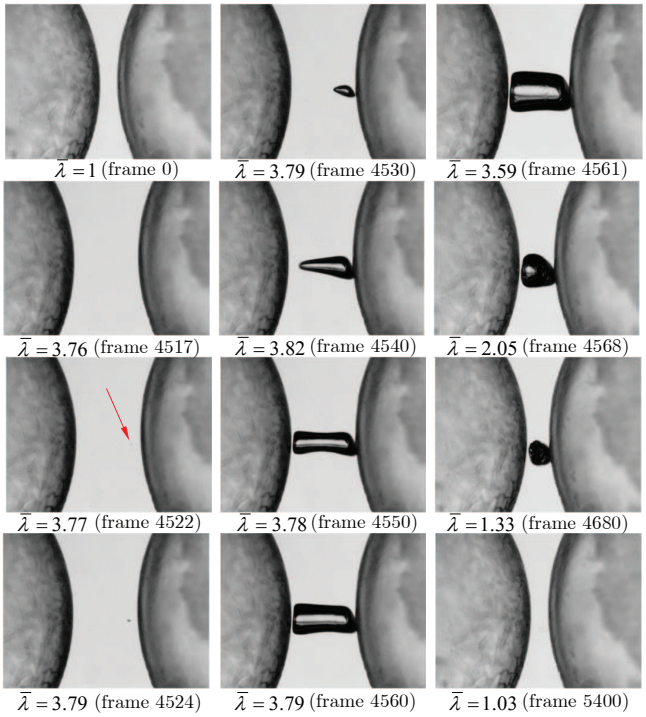

Fig. 2 Selected frames from cycle 1 loading-unloading of the PDMS 30:1 specimen.

During the first loading cycle (see first segment of Video L0-L1 in Electronic Supplementary Information), the average stretch $\overline{\lambda}$

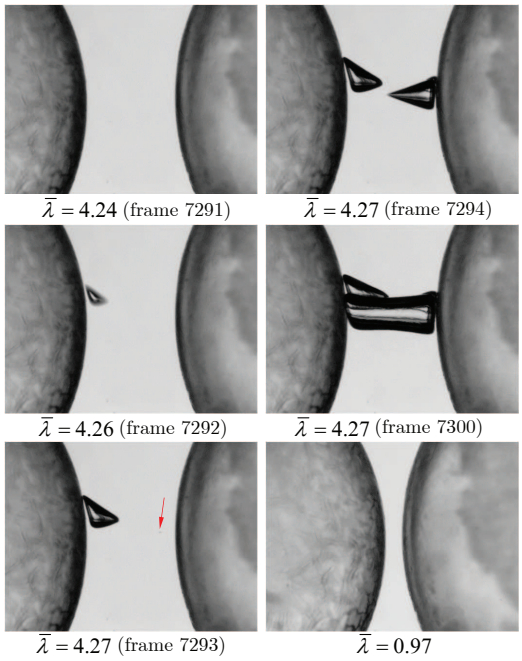

Fig. 3 Selected frames from cycle 2 loading-unloading of the PDMS 30:1 specimen.

between the beads increases monotonically from 1 to 3.82. Selected images from this cycle are shown in Fig. 2. When $\overline{\lambda} = 3.77$, the first cavity/crack nucleates at about 73 μm from the right bead interface almost on the line of symmetry; this is highlighted by the red arrow in Fig. 2. Again, its visibility is due to the occlusion of light. At this stage, the size of the cavity/crack is already about 2 μm in diameter. Upon further loading, this object grows significantly in size and takes a conical or tear-drop shape; as explained further below, this corresponds to nothing more than the deformed configuration of a penny-shaped micro-crack. As this occurred, with the average stretch reaching $\overline{\lambda} = 3.82$, the loading was stopped and then reversed quickly. This reversal was not fast enough, and the conical shape transitioned into a larger cylindrical shape that eventually extended to fill the space between the two beads; as we will demonstrate later, this also corresponds to the deformed shape of a larger penny-shaped crack. With continued unloading, as seen in the images in the right column of Fig. 2, the crack begins to decrease in size, but with a shape that looks different from the cylindrical or conical shapes observed during the loading (nucleation/propagation) portion; this could possibly indicate a break in the axisymmetry of the problem. When the beads are returned to their original position, as seen in the last frame of the right column of Fig. 2, the PDMS region containing the crack is then completely transparent, and there is no optical evidence of the damage that occurred during this cycle L0-L1. At that stage, it was conjectured that the crack had closed, and perhaps healed completely. Note that this is an interior crack, completely embedded within the PDMS and hence was not exposed to contaminants in the surrounding environment (in this case, the atmosphere).

After the first loading cycle, within a delay of less than 2 min-

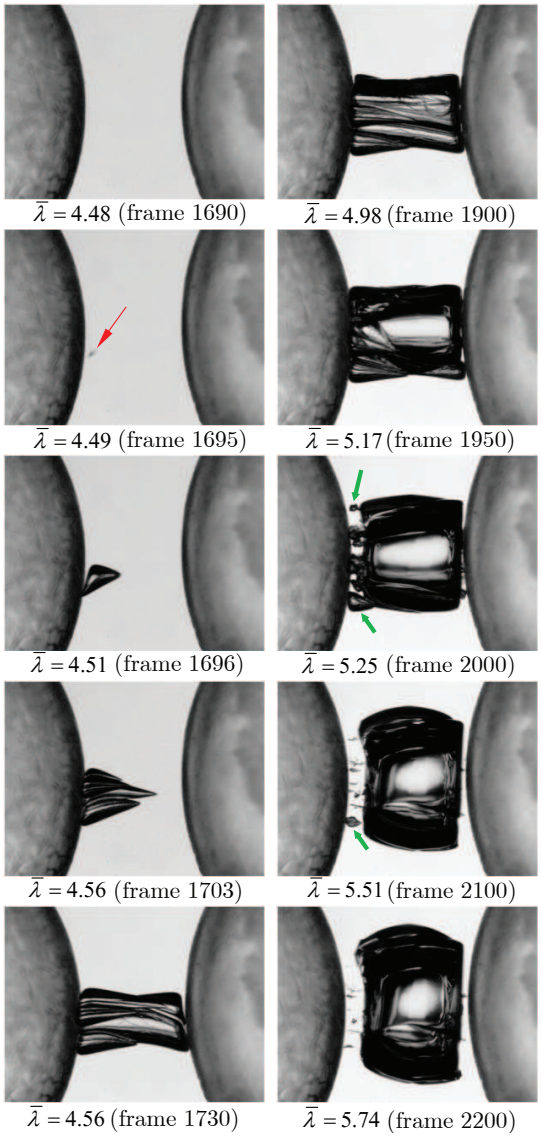

Fig. 4 Selected frames from cycle 3 loading of the PDMS 30:1 specimen.

utes, the second loading cycle (also contained in Video L0-L1) was initiated with the same objectives. Selected images from this cycle are shown in Fig. 3. Surprisingly, when the average stretch exceeds $\overline{\lambda} = 3.77$, the level at which nucleation was observed in cycle L0-L1, there was no evidence of any damage (as inferred from the light transmission characteristics) at the site of the first nucleation! In fact, only when the stretch reaches $\overline{\lambda} = 4.24$, does a cavity/crack nucleate within the specimen, but this time about 57 μm away from the left bead surface, and about 180 μm above the line of symmetry. As this micro-crack continues to grow, a second cavity/crack nucleates at about 102 μm away from the right bead surface when the stretch reaches $\overline{\lambda} = 4.27$ (indicated by the red arrow), almost on the line of symmetry. It should be noted that this is near but not the same location of nucleation during the first loading cycle. Once again, the loading was quickly halted; however, the second crack grew in an unstable manner before arresting as seen in the next image in Fig. 3. Upon unloading, both cracks closed initially from unloading, and eventually disap-

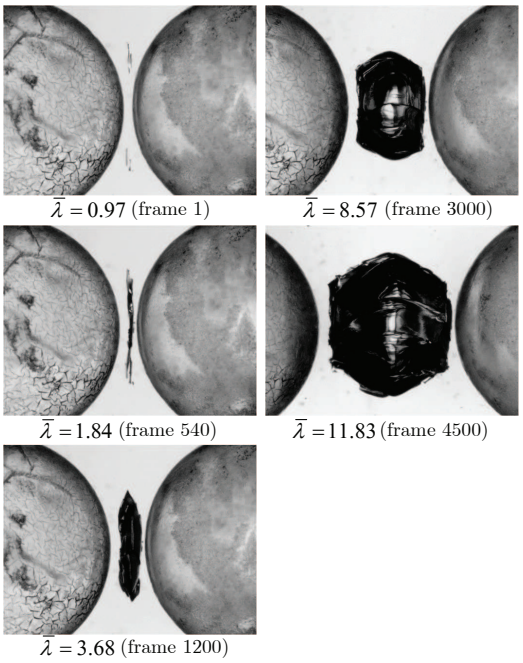

Fig. 5 Selected frames from cycle 4 loading of the PDMS 30:1 specimen.

peared completely, leaving a fully transparent material, with no optical trace of the damage as seen in the last image in Fig. 3.

Now, for cycle 3 (shown in Video L1-L2 of the Electronic Supplementary Information) the same strategy was adopted; the corresponding images are shown in Fig. 4. It appeared that all traces of previous damage were erased. During cycle 3, nucleation thresholds from the previous cycles were exceeded, and the first nucleation of damage appeared when $\overline{\lambda} = 4.49$, at about 51 μm from the left bead surface, about 190 μm below the line of symmetry, i.e., *not* at any of the earlier nucleation sites. With continued stretching, many more nucleation events occur between stretches of $\overline{\lambda} = 4.51$ to $\overline{\lambda} = 4.56$, but it is difficult to count them due to their stacking one behind the other. Loading was continued to explore the further development of these multiple micro-cracks. At average stretches in the range $\overline{\lambda} \in [4.98, 5.25]$, the nucleated micro-cracks may have merged or coalesced into one single entity that could be called a macro-crack. More likely, one micro-crack takes over and the remaining micro-cracks are left unloaded. This latter view could be supported by examining the images corresponding to $\overline{\lambda} = 5.25, 5.51$, and 5.74. The green arrows point to locations where nucleated micro-cracks are in the process of closing and/or healing. After the macro-crack spanned the region between the beads, the specimen was unloaded. It should be recognized that this macro-crack has yet to break through the top and bottom free surfaces of the specimen, and hence is still an internal crack.

Upon unloading, it was difficult to close the crack and thus to heal it completely. This can be seen from the first image in Fig. 5 that shows images from the early stages of loading cycle 4 (Electronic Supplementary Information Video L2-Lf). Waiting over a span of a few minutes did not help to close the crack completely. With continued loading for cycle 4, the crack begins to open, just

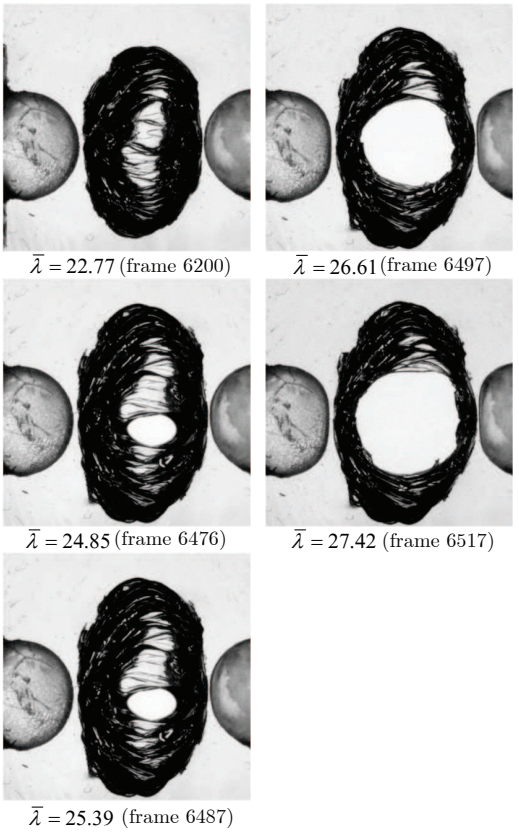

Fig. 6 Selected frames from cycle 4 (segment 2) loading of the PDMS 30:1 specimen.

from the mechanical deformation of the surrounding material, as seen in Fig. 5. Note that the magnification of the images is smaller than in the previous figures in order to display the larger displacements sustained; the bead diameter ($D = 3.170$ mm) provides the scale of the images. The shape seen at $\overline{\lambda} = 11.83$ is the opening of a penny-shaped interior crack that lies along some line between the two beads as seen at $\overline{\lambda} = 1.84$. With continued loading, as shown in Fig. 6, the central part of the macro-crack breaks through the top and bottom free surfaces of the specimen and forms a true through-crack; at this stage, there is no material in this central region and we see a fully open crack. The further evolution of this crack can be seen in the remaining images in Fig. 6. From these images it could be conjectured that perhaps the interior cracks had ligaments or membranes bridging the micro-crack surfaces, but the optical images do not provide adequate resolution to confirm such a conjecture.

4 Discussion

The observations and measurements reported above bring to the fore the core attributes of the processes of nucleation, deformation, propagation, and healing of cavities and cracks in elastomers subjected to externally applied quasistatic loads. Those related to nucleation, deformation, and propagation were already reported and discussed by Poulain et al.[1]. For completeness, we also discuss them in the sequel. Those related to healing are new altogether.

We begin by remarking that the classical cavitation criterion of Gent and Lindley[4] — which, in the present case, happens to roughly agree with the more general criterion of Lopez-Pamies et al.[5] given by Eq. (1) — indicates that cavitation would first occur at $\overline{\lambda} = 1.09$ on the poles of both beads, when and where the Cauchy hydrostatic pressure $p \doteq (t_1 + t_2 + t_3)/3$ would first reach the critical value $p_{cr} = 5\mu/2 = 0.1262$ MPa (recall that the initial shear modulus of the PDMS elastomer with 30:1 composition is given by $\mu = \mu_1 + \mu_2 = 0.05049$ MPa); these critical values were obtained from the full-field simulation of the elastic response of the pristine specimen under the same loading conditions as those applied in the experiment‡. The theoretical stretch $\overline{\lambda} = 1.09$ vastly underpredicts the stretch measured from the experiment in the first loading cycle, namely, $\overline{\lambda} = 3.77$, as well as those in subsequent loading cycles. Moreover, the location at which cavitation would first occur is also incorrectly predicted by the classical theory. Again, the onset of cavitation in the first loading cycle occurs at about 73 μm from the right bead interface almost on the line of symmetry. The full-field simulation of the elastic response of the specimen indicates that the principal Cauchy stressess at that location when $\overline{\lambda} = 3.77$ are given by $t_1 = t_2 = 1.0136$ MPa and $t_3 = 1.8477$ MPa, which far exceed those predicted by Eq. (1).

Now, in order to identify the source of the disagreement between the theoretical *elastic* criterion (1) and the experimental observations for the onset of cavitation, it is helpful to estimate the stretch levels that would be required in the interior surface of the first observed cavity/crack were this to have been solely created by mechanical (elastic or otherwise) deformation. To that effect, let us consider that the intrinsic defects (perhaps free volume defects arising from packing deficiencies) from where cavitation initiates are equiaxed and on the order of 100 nm at most; recall that the imaging of the specimen in its initial configuration confirmed that whatever defects are present from the outset are necessarily submicron in size. A standard calculation then allows one to deduce that, when the cavity/crack is first visible in the experiment at $\overline{\lambda} = 3.77$, its inner surface would have experienced a roughly biaxial stretch of at least 10, but probably much greater since defects in elastomers are typically expected to be at most a few tens — and *not* a few hundreds — of nanometers in size (see, e.g., Gent[10]). Given the non-Gaussian stiffening response of the PDMS elastomer used in the experiment, it is unlikely that such a large mechanical deformation is possible prior to fracture. Thus, as already found in a plurality of other experiments by Poulain et al.[1], the onset of cavitation observed at $\overline{\lambda} = 3.77$ during the first loading cycle is not a purely elastic phenomenon, but one that depends fundamentally on the non-Gaussian stiffening of the PDMS elastomer (i.e., not just on its initial shear modulus μ) and, more significantly, on its fracture properties. Moreover, the random locations at which the onset of cavitation occurs during the first three loading cycles in the experiment, and the increase in the stretch at which cavities/cracks nucleate, point to the fundamentally stochastic nature of the underlying defects from where cavitation initiates, a feature also not accounted for by Eq. (1).

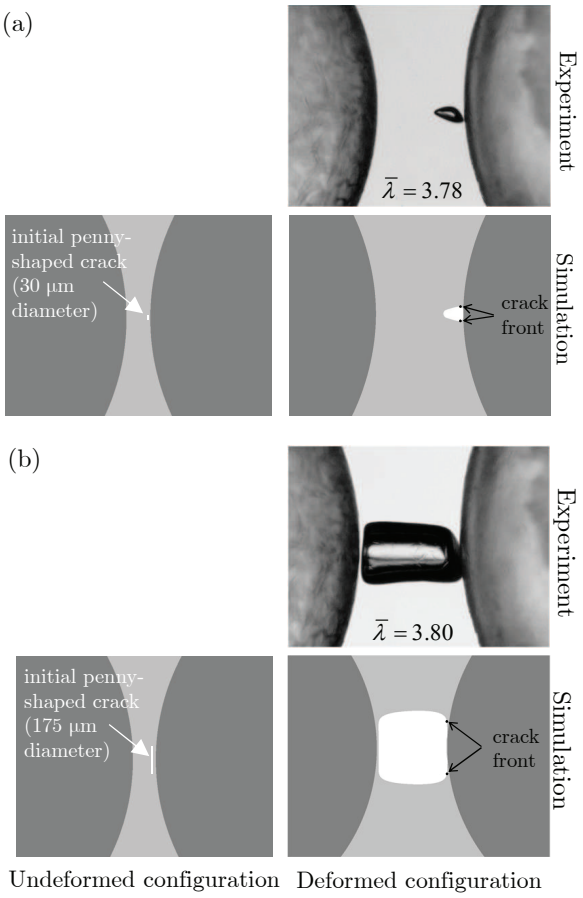

Fig. 7 . Full-field elastic simulation of the experiment shown in Fig. 2 for a specimen containing a penny-shaped micro-crack of (a) 30 μm diameter and (b) 175 μm diameter near the pole of the right bead.

Right after the nucleation stage at $\overline{\lambda} = 3.77$, when $\overline{\lambda} = 3.78$, the cavity/crack is seen to quickly evolve into a conical or teardrop shape of much larger size. Upon further loading, this conical object evolves into one of cylindrical shape and even larger size. As already recognized by Poulain et al.[1], these shapes and sizes are the direct consequences of the propagation of the nucleated cavity/crack into a penny-shaped crack and its subsequent large deformation. The full-field elastic simulation shown in Fig. 7(a) corroborates that the conical shape and size observed in the experiment at $\overline{\lambda} = 3.78$ corresponds indeed to the deformed configuration of a penny-shaped crack of about 30 μm in diameter. Similarly, Fig. 7(b) shows that the cylindrical shape and size observed in the experiment at $\overline{\lambda} = 3.80$ corresponds to the deformed configuration of a penny-shaped crack of about 175 μm in diameter.

Having examined the nucleation, deformation, and propagation of the cavity/crack observed in the experiment during the first loading cycle, we now turn our attention to the events observed during the unloading and subsequent reloading of the specimen. Again, upon the first unloading, the crack nucleated near the right bead heals completely. It does so by following a different path than the one followed during its nucleation and

‡ The interested reader is referred to Section 4 in Lefèvre et al.[9] for details of such a type of simulations.

propagation. At this point, we do not know the molecular mechanisms responsible for such healing. Clearly, one must examine the role, if any, of the lower cross-link density when compared to the standard PDMS composition recommended by the manufacturer. For example, the possible presence of untethered PDMS chains could potentially influence the healing response observed and needs to be explored further. In this context, the present observations should be contrasted with work in two different directions. First, increasing efforts have been devoted in recent years to the investigation of crack healing in elastomers featuring sophisticated chemistries that promote healing [11–13]. Second, there has also been significant work in the fracture of viscoelastic fluids [14–16]; these focus on external cracks in polymer liquids, while the present work has been concerned exclusively with internal cracks in an elastomeric solid. The remarkable finding in the present work is that internally nucleated cracks in a conventional elastomer can heal completely, without sophisticated chemistries to influence bonding interactions, and even when they have grown to be tens of microns in length scale, in a time scale of seconds.

Upon reloading, as shown in Figs. 3 and 4 for the second and third loading cycles, the onset of cavitation occurs at the larger stretches $\overline{\lambda} = 4.24$ and $\overline{\lambda} = 4.49$, respectively. Associated with this is a significant increase in the hydrostatic pressure at the locations of nucleation, which in turn implies a "strengthening" or "toughening" of the material with load cycling. Such strengthening may be rationalized in terms of the stochastic nature of the underlying defects together with the development of residual stresses as follows. During the first loading, the defect that meets the cavitation criterion the earliest gets nucleated into a micro-crack before all others. During the first unloading, there is insufficient time for the PDMS to retract to its equilibrium state; this results in a non-equilibrium packing at a higher volume, and potentially a residual compressive stress in the vicinity of this first defect. Hence during subsequent loading cycles, this defect no longer reaches criticality first. Instead, during the second loading segment, nucleation occurs at the second defect that meets the cavitation criterion, and as we see in the experiments, this is at a different physical location and at a larger loading. This second defect, upon unloading, becomes stronger by the same mechanism outlined above and, consequently, it does not nucleate during the third loading cycle. As we move through loading-unloading cycles, the tail of the distribution of defects is probed, and hence we anticipate more defects to reach criticality. This is precisely what is observed: at a stretch of $\overline{\lambda} = 4.98$ during cycle 3, as shown by Fig. 4, there are indeed numerous micro-cracks that get nucleated.

The unloading of the specimen in cycle 3 does not lead to the complete healing of all the various cracks that were nucleated. It is unclear whether they would have healed had the specimen not been reloaded a fourth time. As the applied load is increased in cycle 4, a macro-crack with dimensions comparable to the bead spacing is formed. There appear to be two possible mechanisms in the observed macro-crack development: either several of the different micro-cracks coalescence to form a macro-crack or there is a competition between them and one emerges as the macro-crack, while the rest are arrested and heal. Exploring the behavior during cycle 3 in Fig. 4, as the average stretch increases from $\overline{\lambda} = 5.25$ to $\overline{\lambda} = 5.74$, it is seen that one crack begins to dominate, and as this grows, the remaining micro-cracks appear to be unloading and healing (closing). These observations suggest that the macro-crack is formed by the propagation of a single micro-crack and not by the coalescence of several of them.

5 Summary and conclusions

Experiments were performed at high spatiotemporal resolution to explore the details of the internal nucleation and propagation of fracture and healing in a transparent PDMS elastomer subjected to externally applied mechanical loads. This was accomplished by confining a region of the PDMS between two firmly embedded stiff beads and stretching the specimen along the line of symmetry connecting the centers of the beads, in the same spirit as in the original work of Gent and Park [2]. The monotonically (first) increasing and (then) decreasing load, applied cyclically, led to a controlled nucleation, propagation, and healing of cavities/cracks in the PDMS region confined between the beads. All these processes were directly observed at high resolution through an optical microscope. The main observations pertaining to the nucleation and propagation of fracture were originally reported by Poulain et al. [1], but we also summarize them here for completeness:

- Optically visible fracture appears in regions of the PDMS where the hydrostatic part of the stress is high, but the strain is small. The internally created new surfaces correspond roughly to penny-shaped cracks that in the deformed configuration take the form of tear drops or cylinders, this depending on their size relative to the diameter of the beads and the gap between them.

- The nucleation of fracture depends fundamentally on: (*i*) the non-Gaussian stiffening of the PDMS, (*ii*) on its fracture properties, and (*iii*) on its inherent defects. Consequently, elastic cavitation criteria that only depend on the initial shear modulus of the elastomer under investigation, and that do not account for its fracture properties or for the stochastic nature of its defects, are not able to describe or predict the nucleation of fracture in this class of PDMS elastomers.

The main observations pertaining to the healing of the PDMS during the repeated loading and unloading of the specimen are as follows:

- Internally nucleated cavity/cracks can completely heal, even when they have grown to be tens of microns in length, in a time scale of seconds. This healing occurs autonomously, without the application of any external stimulus (e.g., heat).

- The regions of the PDMS elastomer that experience healing appear to exhibit significant strengthening or toughening, resulting in the nucleation of cavities/cracks occurring at increased loading levels elsewhere in the PDMS during subsequent loading cycles. This behavior hints at an evolution of the underlying molecular rearrangement and/or chemical bonding due to the healing process.

- Significant variations were observed in the locations and critical stretch levels at which the nucleation of cavities/cracks occurred during subsequent cycles. This observation further supports the relevance of the stochastic nature of defects in the process of nucleation of fracture.

Conflict of interest

There are no conflicts to declare.

Acknowledgements

This work was performed during the course of a collaborative investigation into cavitation, fracture, and damage in soft materials funded by the National Science Foundation collaborative grants CMMI–1235352 and CMMI–1235138. This support is gratefully acknowledged.

References

1 X. Poulain, V. Lefèvre, O. Lopez-Pamies and K. Ravi-Chandar, *International Journal of Fracture*, 2017, **205**, 1–21.

2 A. N. Gent and S. Park, *Journal of Materials Science*, 1984, **19**, 1947–1956.

3 O. Lopez-Pamies, M. I. Idiart and N. Nakamura, *Journal of the Mechanics and Physics of Solids*, 2011, **59**, 1464–1487.

4 A. N. Gent and P. B. Lindley, *Proceedings of the Royal Society A*, 1959, **2**, 195–205.

5 O. Lopez-Pamies, N. Nakamura and M. I. Idiart, *Journal of the Mechanics and Physics of Solids*, 2011, **59**, 1488–1505.

6 M. L. Williams and R. A. Schapery, *International Journal of Fracture Mechanics*, 1965, **1**, 64–71.

7 P. Flory, *Principles of Polymer Chemistry*, Cornell University Press, Ithaca, 1953.

8 O. Lopez-Pamies, *Comptes Rendus Mecanique*, 2010, **338**, 3–11.

9 V. Lefèvre, K. Ravi-Chandar and O. Lopez-Pamies, *International Journal of Fracture*, 2015, **192**, 1–23.

10 A. N. Gent, *Rubber Chemistry and Technology*, 1990, **63**, 49–53.

11 P. Cordier, F. Tournilhac, C. Soulie-Ziakovic and L. Leibler, *Nature*, 2008, **451**, 977–980.

12 B. J. Blaiszik, S. L. B. Kramer, S. C. Olugebefola, J. S. Moore, N. R. Sottos and S. R. White, *Annual Review of Materials Research*, 2010, **40**, 179–211.

13 F. B. Madsen, L. Yu and A. L. Skov, *ACS Macro Letters*, 2016, **5**, 1196–1200.

14 H. Tabuteau, S. Mora, G. Porte, M. Abkarian and C. Ligoure, *PRL*, 2009, **102**, 155501.

15 H. Tabuteau, S. Mora, M. Ciccotti, C.-Y. Hui and C. Ligoure, *Soft Matter*, 2011, **7**, 9474.

16 Q. Huang, N. Alvarez, A. Shabbir and O. Hassager, *Physical Review Letters*, 2016, **117**, 087801.

Damage in elastomers: Healing of internally nucleated cavities and micro-cracks

Xavier M. Poulain, Oscar Lopez-Pamies, Krishnaswamy Ravi-Chandar

Cavities and micro-cracks self-heal completely!